Experimental Study of Different Materials on Electromagnetic Damping Characteristics

M.F. Mohd Yusoff[a*], A.M. Ahmad Zaidi[b*], S.A. Firdaus Ishak[a], M.K. Awang[a], MF Md Din[a], A. Mukhtaruddin[a], A.M. Ishak[a]

[a]*Faculty of Engineering,*
National Defence University of Malaysia,
[b]*Faculty of Defence Science and Technology,*
National Defence University of Malaysia,
Sg. Besi Camp 57000 Kuala Lumpur, Malaysia

[*]*Corresponding author: fazli@upnm.edu.my; mujahid@upnm.edu.my*

Abstract **— Electromagnetic damper (EMD) is an alternative approach in a suspension system. It has been investigated through simulation and experimental means. Since the effect of a damper is closely related to the vibration system, the dynamic characteristics of the system can be acquired by analysing the vibration response of the EMD. This paper presents an investigation of the EMD effect through a simulation and experimental study. The EMD system was simulated in MATLAB by considering the system as a mass-spring-damper system. A vibration test rig with a simple EMD was fabricated and tested to investigate the effect of electromagnetic force. Results showed that the vibration system test rig can operate as a free vibration system or a forced vibration system. It was also confirmed that aluminium has a better damping coefficient value (2.8 kgs^{-1}) as compared to nylon (1.9 kgs^{-1}) as an outer cylinder of the EMD system. The damping coefficient is directly related to the material used in the damper, such that the amplitude and settling time of the vibration system can be reduced accordingly.**

Keywords **— Electromagnetic damper; eddy current; vibration; suspension system; MATLAB.**

Manuscript received 15 Oct. 2020; revised 29 Jan. 2021; accepted 2 Feb. 2021. Date of publication 17 Feb. 2021.

I. INTRODUCTION

Problematic issues in vibration, such as fracture, energy loss and fatigue, in a suspension system are the subject matters that need to be addressed by an engineer. Engineers tackle these issues by improving the vibration damping response and adjusting the isolation system. Undesirable vibration will cause damage or fracture to a system, for example, the excessive vibration presented in a car will induce harmful wear on the components of the car [1]. Traditionally, the damper and spring system is the main element investigated in a suspension system of a vehicle to obtain the best performance of a car in terms of ride and handling, as well as to withstand the weight of the car.

Vibration and suspension are two elements that are very common in a suspension system. Suspension can be categorised into passive, semi-active and active systems. While each type of system has its advantages and disadvantages, most researchers are in favour of the semi-active system since the passive system can be tuned only during the manufacturing process, whereas the active system tends to be complex and costly.

Suspension is categorised into the active system, passive system and semi-active system based on the level of controllability [2]. The classification of suspension systems is based on their capability to take in, contribute to or remove energy. The basic elements in a suspension system are the spring and damper units. The main types of suspension systems being used in the current automotive industries are hydraulic and pneumatic devices [3].

According to studies, the conventional passive suspension has an absorber as a damper and a spring to communicate with sprung mass and unsprung mass [2,4]. The response of this system depends on the damping and spring constants that have been fixed during the set-up [5].

A suspension system consists of a sprung mass (car chassis on top of spring), an unsprung mass (any mass related to the linkage system located below the spring) and a spring and damper system. The spring stores energy, the shock absorber dissipates energy proportional to its damping coefficient and the links restrict the suspension system and limit motion [6]. A suspension system is used as part of the vehicle system because it has several tasks to perform during the movement of the vehicle. The tasks, including providing a smooth ride by shielding the vehicle body from road imperfections, improving ride handling by maintaining constant wheel-to-road contact and supporting the vehicle weight, are all competing demands for a suspension system [6]. Good handling requires a suspension setting that is neither too stiff nor too soft. On the other hand, a comfortable ride can be achieved by having a soft suspension. However, an overly soft suspension is not able to respond instantly to any load variation. Thus, a balance between the two opposing requirements needs to be taken into account by a suspension designer, as illustrated in Figure 1.

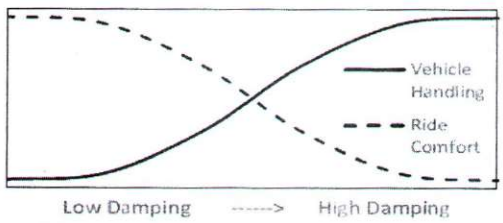

Figure 1: Vehicle handling and ride comfort in passive suspension [7]

Typically and traditionally, hydraulic and pneumatic devices are used and implemented in a vehicle suspension system [3,8], which have several drawbacks like hose leaks and ruptures. Such a system is also inefficient due to the required continuously pressurised system [9].

Thus, an alternative way to avoid all the issues pertinent to hydraulic usage is electromagnetic damping, which is an oil-free, no mechanical contact, high reliability and stability approach that is applicable in various vibration isolation systems, including micro-mechanical suspension systems, structure vibration isolation systems and precision machinery [10,11,12].

In a recent study, an eddy current damper (ECD) was developed and analysed using finite element analysis [12]. The research was further analysed through MATLAB simulation by investigating the effectiveness of the ECD in a quarter-car system. The results of the simulation with and in absence of the ECD were analysed. Essentially, the effect of electromagnetic can be divided into two phases. The first effect is due to the eddy current induced in the system by considering Faraday's law. The second effect that can be tested under this concept is by creating a solenoid such that it will interact with the permanent magnet.

When a moving conductor crosses a stationary magnetic field or vice versa, eddy currents are generated. Eddy currents circulate within the conductor because of the magnetic fields and the relative velocity of the conductor. The instantaneous creation of an opposing magnetic field by the movement of electrons in the conductor results in Lorentz forces, which dampen the motion of the magnet and generate heat within the conductor [13,14]. A resistive force is developed as the eddy current circulation induces a magnetic field [15].

Even though eddy current can be used as a damper, there are still some issues that need to be addressed, such as magnetic contamination and heat generation [14]. Additionally, such a system increases the volume of the suspension since the force density of the active component of the hydraulic system is larger than that of electromagnetic actuation, and it raises system costs because permanent magnets are more costly [16]. Thus, the use of electromagnetic damper (EMD) needs to be investigated whether it can benefit or be harmful to any dedicated system. In this research, the effect of different materials as the EMD was investigated experimentally by using a one-degree-of-freedom (1DOF) vibration test rig.

II. *General concept of electromagnetic damper*

Various research and development were related to electromagnetic damping [1,3,11,17,18]. Eddy currents are one example of electromagnetic induction; their effects can be applied in an ECD. It has been reported that the life of the damper can be prolonged because it is a non-contact damping device which does not need to have physical contact. It will also not have an issue due to the fluid seal and leakage. On top of that, regenerative energy can be generated because of the interaction of magnetic flux from the magnet and the conductor around it [19].

In order to regulate the vibrations of a tiny cantilever beam, Sodano et al. [20] examined the use of an ECD. On the other hand, other researchers studied the application of ECD as a vibration control system in vehicles and structures [12,14,21-31].

Gysen et al. [16] investigated the presence of linear motors in an active electromagnetic suspension (EMS). In their paper, a quarter-car 1DOF experimental setup was deployed with a tubular permanent magnet actuator, as shown in Figure 2.

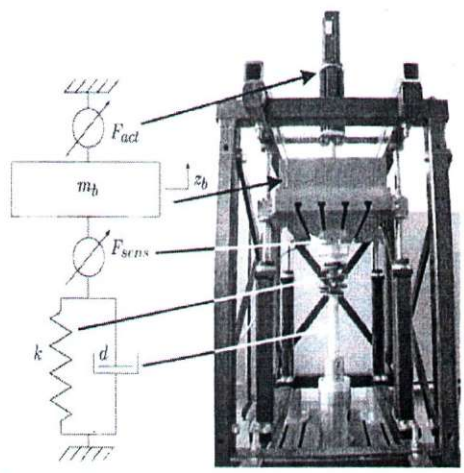

Figure 2: Quarter-car test setup and its schematic diagram [16]

By adding external voltage to the armature winding, the thrust force can be actively produced. The permanent magnet translator is subsequently impacted by the active armature, resulting in a linear movement.

Asadi et al. [32] created an adaptive and regenerative damper prototype that is referred to as a hybrid EMD. The hybrid damper is set up to work with electromagnetic and viscous subsystems. The electromagnetic component was modelled, examined physically and analysed using an analytical (lumped equivalent magnetic circuit) and finite element method software, namely COMSOL. According to the modelling and testing data, the damper can yield electromagnetic damping viscous coefficients of 1,300 Nsm^{-1} and 0-238 Nsm^{-1}, respectively.

Montazeri et al. [33] studied the ideas on how to generate energy and create a damping effect from relative motion between sprung and unsprung masses. The EMD can be used as a damping element to isolate a system from a vibration source, and at the same time, generate energy. The implementation of the ideas was done by considering the EMD as a passive damper in a quarter-car model. The output of the simulation showed that the passive EMD was able to generate electricity while fulfilling the basic task of a suspension system.

A 1DOF vibration isolation system test rig was developed such that an ECD can be tested [34]. The ECD was designed

with the permanent magnet design arrangement in mind. The electromagnetic equations were used to develop an analytical model of the induced eddy current force. The prototype of the system was created and tested, revealing a tenfold increase in damping characteristics of a 1DOF isolation system.

In the study of Fow and Duke [35], the authors developed and validated a small-scale passive linear EMD by employing a permanent magnet and coil arrangement. It was then tested in a 1DOF system test rig, as depicted in Figure 3 below.

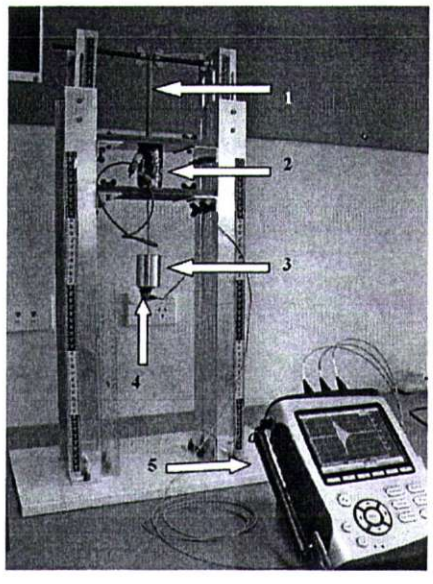

Figure 3: A small test rig constructed for initial validation of the damper model [35]

The magnet and coil constituted the damping in the system; the magnet and coil were modelled numerically as an air-cored solenoid. The numerical model of the passive damper was derived using the Biot-Savart law equation. As the masses moved vertically in the test rig, the flux generated was determined and recorded in a lookup table such that the dynamic model can be created. Later in the research, the dynamic model was scaled up to be applied as an EMD in a quarter-car model. A damping coefficient of 1,600 Nsm^{-1} was achieved in the two-degree-of-freedom quarter-car model. However, the volume needed for the developed system increased more than threefold as compared to equivalent hydraulic dampers [35].

In another study, a control algorithm utilising an H∞ controller was used in conjunction with the designed linear motor model such that an active suspension system can be materialised [24]. The controller controlled the amount of electric power needed to be supplied during the operation. On the other hand, an analytical model of a non-laminated axisymmetric cylindrical electromagnetic suspension system was developed by considering six elements in the rotor, coil and flotor design [36]. A fractional order system was obtained in the transfer function by considering the flotor position as the output and the perturbation current as the input to the system.

Moreover, a rack-and-pinion-based regenerative EMD was developed and tested experimentally [37]. The dynamic modelling of the system was done by considering an electric motor as a generator such that a steady power of voltage can be captured. The research was further prolonged by having a prototype in the experimental work. The findings of the experiment showed that a voltage was generated with an average power of 19.2 W and a peak power of 67.5 W. This experiment was conducted on a smooth campus road when the car was moving at 48 km/h (30 mph).

The basic idea of this research was to create a magnetic flux interaction between the permanent magnet and the hollow cylinder which surrounded the permanent magnet movement. The permanent magnet moved vertically through the EMD (a copper coil-wounded hollow cylinder), as shown in Figure 4.

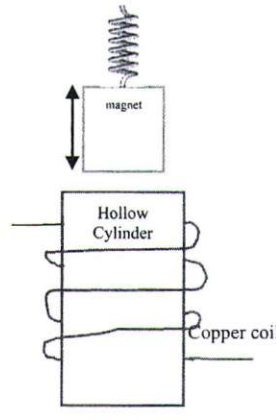

Figure 4: Schematic diagram of the main source of EMD effect

A ring-shaped ferrite magnet attached to an aluminium rod acted as a translator moving through the hollow cylinder wounded with copper coil. Thus, the magnetic field varied such that an electromagnetic induction was induced into the wounded cylinder. The changing magnetic field generated eddy currents into the hollow cylinder, as proven by Michael Faraday [35,38,39]. Michael Faraday created Faraday's law which indicates that the induced voltage increases with the magnetic flux density and the rate of change of the magnetic flux linkage [40]. The equation can be expressed as:

$$V_{emf} = -N\frac{d\emptyset}{dt} \quad (1)$$

where N refers to the number of revolutions of the coil in the circuit which is considered an N-turn filamentary conductor of the closed path and ϕ is the magnetic flux (in unit Weber) through each turn.

The negative sign is based on Lenz's law which states that an induced electromotive force produces a current opposing the direction of the change of magnetic flux that induces it. Figure 4 shows the magnets moving up and down in the coil. According to Faraday's law, the change in magnetic flux will induce an electromagnetic force in a closed circuit. Therefore, the changing magnetic flux due to the moving magnets repeatedly will produce an alternating voltage in the coils. From that, magnetic flux, ϕ, is defined as the number of magnetic field lines passing through a given closed surface, expressed as:

$$\Phi = \int_s B.dS \quad (2)$$

where B is the magnetic flux density in the unit of Tesla and dS is the element of the surface [40].

Based on the Maxwell-Faraday equation, electromagnetic induction can be explained. The Maxwell-Faraday equation states that:

$$\nabla \mathrm{x} \vec{E} = -\frac{\partial B}{\partial t} \quad (3)$$

which means the partial derivative of the magnetic field is equal to the curl of the electric field.

Integrating this equation over a plane surface:

$$V_{emf} = \oint \boldsymbol{E} \cdot d\boldsymbol{L} = -\frac{d}{dt}\int_S \boldsymbol{B} \cdot d\boldsymbol{S} \quad (4)$$

The result will be an electric field in the contour of the area equal to the changing of magnetic flux responding to time; both sides of the equation are equal to a voltage. This shows that the electric current or voltage can be produced with a changing magnetic field within a stationary loop or a constant magnetic field within a moving loop [40].

The force between the magnet and electromagnet can be considered as:

$$F = \int_\Gamma J \times B \, d\Gamma \quad (5)$$

where B, J and Γ are magnetic flux density, induced current density and the conductor's volume, respectively.

Assuming a constant magnetic flux density in the designated area, the induced current density, J, in the conductor can be calculated as follows:

$$J = \sigma(VXB) \quad (6)$$

This equation indicates that the induced current density (J) will be affected by the conductivity of the medium (σ), flux density (B) and the relative vertical velocity between the stator and the conductor (V).

Thus, based on the Lorentz force law, the eddy current was created in the conductor due to the relative movement of the magnet and conductor. A magnetic flux was produced in an opposite direction to oppose the external magnetic flux density, which in turn, resulted in a damping effect in the system [41].

A. *Damping ratio, ζ*

The decay of oscillations in a vibration system is known as the damping ratio, ζ (zeta). The rate of decay of oscillations between each bounce is measured by the damping ratio. The damping ratio can be categorised into undamped ($\zeta = 0$), underdamped ($\zeta < 1$), critically damped ($\zeta = 1$) or overdamped ($\zeta > 1$). In this experiment, the damping ratio was determined through logarithmic decrement because the system was underdamped.

The vibration response was analysed by looking at the oscillation period, T. The oscillation period is defined as the interval time between two pinnacle points on the graph. The equation involved is as follows [11]:

$$T = \frac{t_n - t_0}{n} \quad (7)$$

where t_n refers to the time when the nth peak occurs as shown in Figure 5.

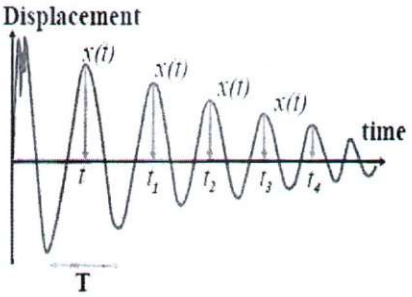

Figure 5: Response of a typical damped system [11]

The logarithmic decrement can be obtained using the following equation [14]:

$$\delta = \log\left(\frac{x(t_n)}{x(t_{n+1})}\right) \quad (8)$$

where $x(t_n)$ is a displacement located at the nth peak.

From the T and δ in equations 7 and 8, the damping ratio, ζ, can be calculated as follows:

$$\zeta = \frac{\delta}{\sqrt{4\pi^2 + \delta^2}} \quad (9)$$

B. *Damping coefficient, c*

The damping coefficient of a system refers to the ability of the system to dampen out an oscillation. In general, a bigger value of c will indicate a higher ability of the system to dissipate the energy and cause the oscillation to die out quicker. The damping coefficient can be determined by applying the values of the damping ratio, mass of sprung mass and spring stiffness. Deriving from equation 9, the value of the damping coefficient, c, will be affected by the value of the damping ratio, ζ, as represented by the following equation:

$$\xi = \frac{\delta}{\sqrt{(4\pi)^2+\delta^2}} = \frac{c}{2\sqrt{mk}} \quad (10)$$

where m is the mass, k is the spring stiffness and c is the damping coefficient.

III. *Test method*

In this paper, an experimental approach was used to show the effect of different materials in an EMD. Firstly, a vibration test rig was designed as a mass-spring-damper system. The experimental test was carried out with two different materials, namely, aluminium and nylon. The two types of EMDs constructed from aluminium and nylon were fabricated and tested using the test rig. Figure 6 shows the two EMDs, each with 900 turns of copper wire coil. The copper wire had an insulator around it to prevent a short circuit in the connection. The dimensions of the two cylinders were the same, with 220 mm in length, a 76 mm outer diameter and a 66 mm inner diameter.

Figure 6: Two different cylindrical materials (aluminium and nylon) for electromagnetic damper

The results from the test were extracted and analysed. The parameter of the system was extracted using the logarithmic decrement method. After that, a simulation using MATLAB software was conducted to visualise the effect of the damping coefficient clearly.

IV. *Experimental test rig of electromagnetic damper*

The components of the test rig system are shown in Figure 7. The basic components are the EMD, sensor, spring, linear bearing, permanent magnet, LMS Data Acquisition System and LMS Test Express Software [42]. The spring and linear bearing enabled the system to oscillate vertically once they were excited. A permanent magnet was attached to the end of the shaft. The dimensions of the ferrite magnet were 22 mm (inner diameter), 45 mm (outer diameter) and 8 mm (thickness of each magnet). The vibration response of the system was taken by the accelerometer sensor which was connected to the LMS Data Acquisition System and LMS Test Express Software [43]. The acquired response was the acceleration response of a mass-spring-amper system, which can be integrated to obtain the velocity and displacement responses of the system. The EMD, which was the subject of investigation in this study, was located at the bottom of the test rig, which interacted with the oscillating permanent magnet as the system was being excited.

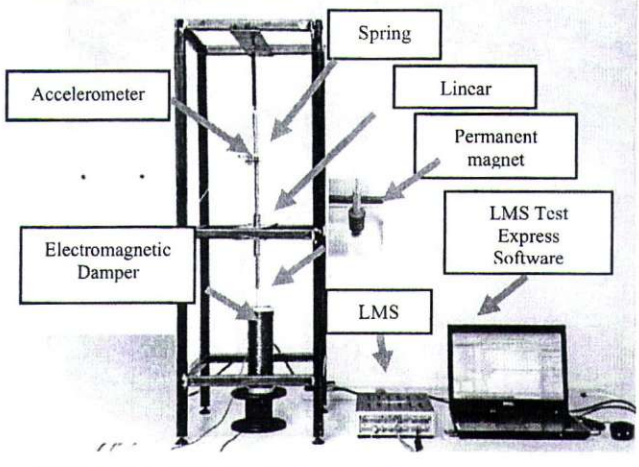

Figure 7: Overview of vibration test rig system

V. Experimental result

Several trial runs were done, and the best result was captured for analysis. Figures 8 and 9 show the responses obtained from the vibration test rig for a 6 cm and 8 cm initial displacement response, respectively. The initial displacement was arbitrarily chosen from the maximum displacement available based on the test rig capabilities. The objectives were to obtain the effect of vibration clearly and illustrate the effect on the EMD through the experiment.

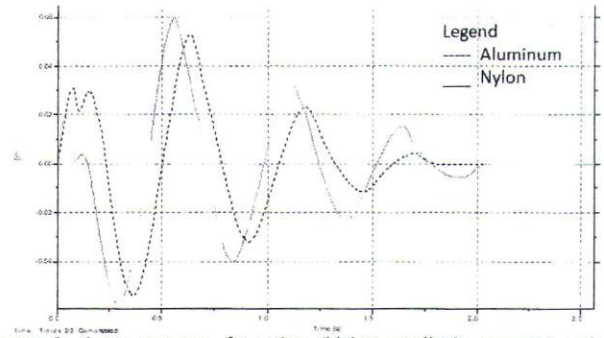

Figure 8: 6 cm response for nylon (higher amplitude response) and aluminium (lower amplitude response)

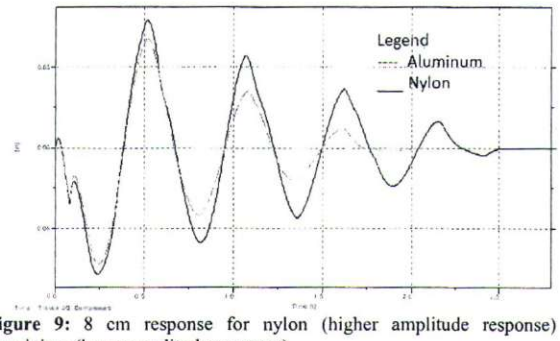

Figure 9: 8 cm response for nylon (higher amplitude response) and aluminium (lower amplitude response)

The data was extracted and analysed to identify the value of the peak using MsExcel. Figures 10 to 13 show the responses from the experiment.

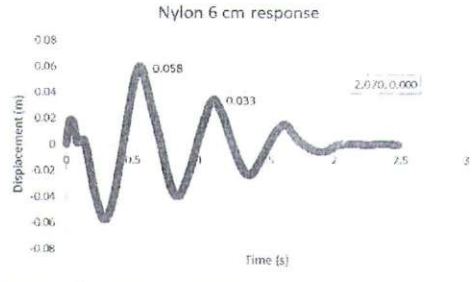

Figure 10: Nylon 6 cm response

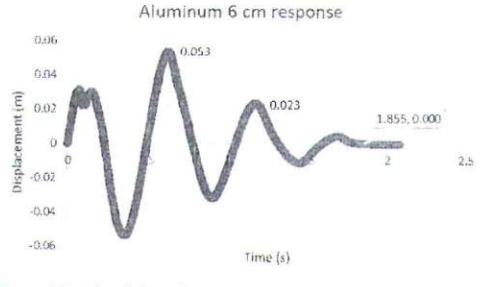

Figure 11: Aluminium 6 cm response

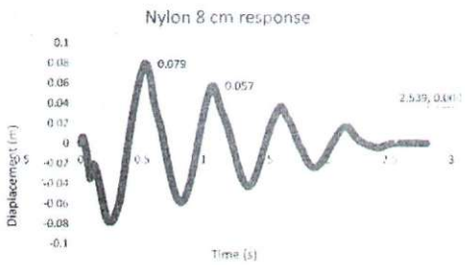

Figure 12: Nylon 8 cm response

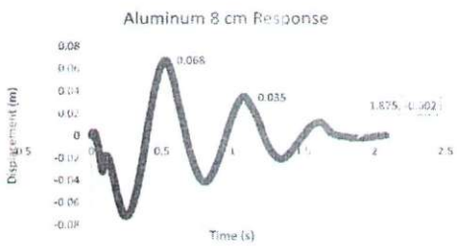

Figure 13: Aluminium 8 cm response

For comparison purposes, all the responses are tabulated in Table 1. Aluminium gave the highest value of damping ratio and coefficient. These were represented by the settling time, damping coefficient and amplitude of the vibration response.

Table 1: Vibration response by materials and amplitudes

Material	Aluminium		Nylon	
Initial amplitude (cm)	6 cm	8 cm	6 cm	8 cm
Logarithmic decrement, δ	0.87	0.67	0.59	0.33
Damping ratio, ξ	0.137	0.106	0.093	0.052
Damping coefficient, c (kgs^{-1})	2.80	2.17	1.90	1.05
Time taken to achieve steady state, t_s(s)	1.85	1.87	2.07	2.54

A. *MATLAB simulation of the vibration test rig system*

The vibration test rig system with the EMD was considered a mass-spring-damper system, as shown in Figure 14.

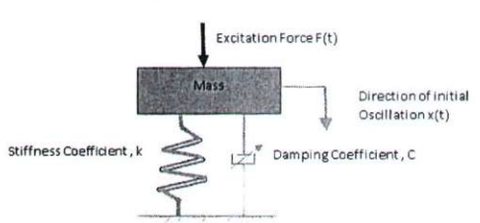

Figure 14: Diagram of a mass-spring-damper system excited by a force

The equation of motion derived based on Figure 14 can be written as follows:

$$\ddot{x} = \frac{1}{m}(F - c\dot{x} - kx) \quad (11)$$

The second-order ordinary differential equation can be represented in the state space form of $\dot{X} = AX + Bu$ by considering the displacement x(t) and velocity $x(\dot{t})$ as the state vector, and the F(t) as the input vector: $X_1(t) = X(t)$, $X_2(t) = \dot{X}(t)$ and $u(t) = F(t)$

Rearranging the equation into a matrix form:

$$\dot{X_1}(t) = X_2(t) \quad (12)$$

$$\dot{X_2}(t) = -\frac{k}{m}X_1(t) - \frac{c}{m}X_2(t) + \frac{1}{m}u(t) \quad (13)$$

This equation can then be represented as a state space equation as follows:

$$\begin{bmatrix}\dot{x_1}\\ \dot{x_2}\end{bmatrix} = \begin{bmatrix}0 & 1\\ -k/m & -c/m\end{bmatrix}\begin{bmatrix}x_1\\ x_2\end{bmatrix} + \begin{bmatrix}0\\ 1/m\end{bmatrix}[u(t)] \quad (14)$$

The effect of damping and spring constant was plotted in the MATLAB software, as shown in Figure 15. The value of the damping constant was affected by the damping ratio, ζ, as illustrated in equation 10 previously. As shown in Figure 15, the damping ratio, ζ, which was directly related to the damping coefficient, c, played an important factor in the vibration response. For instance, the lower value of c (500 Nsm^{-1}) produced an underdamped oscillation response. The amplitude of the vibration decayed over time. In contrast, the bigger value of c (4,500 Nsm^{-1}) produced a response which decayed more quickly than the underdamped response. In short, greater damping caused the energy to dissipate more quickly and prevented the system from vibrating.

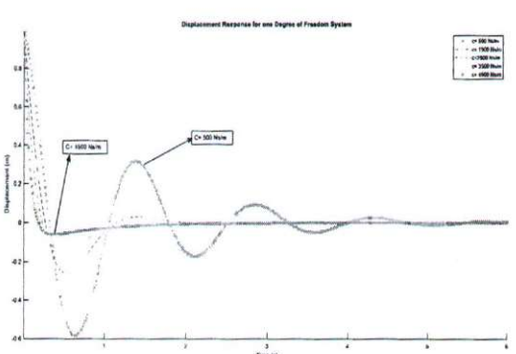

Figure 15: Displacement response for one degree of freedom system

VI. Discussion

The experimental results clearly showed that the value of the damping coefficient affects the vibration response. This relationship is evident from the damping coefficient (c) of the system, as well as the settling time of the response. The settling time for a 6 cm-response aluminium EMD was only 1.85 seconds. In contrast, for a nylon EMD, the time was

slightly longer at around 2.07 to 2.54 seconds. This is in line with the simulation obtained from the 1DOF system using MATLAB which indicated that the vibration response is affected by the damping coefficient (c).

It is also worth noting that the damping coefficient (c) existed in the actual EMD system. This can be proven by looking at the response obtained, as shown in Figures 8 and 9. In other words, the assumption deployed for the MATLAB simulation as per Figure 14 made sense. The damping coefficient (c) was varied so that the vibration response can be controlled. If this result were to be used for a suspension system, the displacement amplitude of the sprung mass can therefore be controlled. A lower amplitude will give less disturbance to the passenger of the car; the passenger will not feel the bouncing effect due to the road condition. Thus, the car will become more stable during the movement of the car and the passenger will be more comfortable while cruising.

From the experimental result, the material of the EMD to be considered should generate a high magnetic flux value. This effect can be related to the permeability of the material, which allows the magnetic lines of force to pass through it. For instance, the permeability value for aluminium is 1.256 μH/m, whereas it is less than 1 for nylon [44], thus, enabling aluminium to create a bigger value of magnetic flux density. The magnetic lines will produce the magnetic flux density, B, as indicated by the following equation [40]:

$$B = \mu_o n I \tag{15}$$

$$n = \frac{N}{L} \tag{16}$$

where L is the length of the solenoid, N is the number of turns of the coil, I is the current in ampere, A, and $\mu_o = 4\pi \times 10^{-7}$ Tesla, T, is the magnetic permeability constant of the magnet in free space.

The novelty of this research lies in relating the vibration system response (mass-spring-damper system) with the electromagnetic damping coefficient (c) effect. The vibration response of the system (displacement response) was analysed with the logarithmic decrement method so that it can be related to the damping coefficient (c) of the system.

From a vibration system point of view, the damping coefficient (c) of a mass-spring-damper system can be obtained from a general equation of:

$$F = cv$$

where $$c = 2\pi a \frac{N^2 B_{rad}}{R} \frac{d\emptyset}{dt} \frac{1}{v}$$

This is the general equation which relates the force of the damping to the damping coefficient (c) and velocity (v). This expression is derived from the effect of the permanent magnet moving vertically towards a coil of wire, as discussed by Saslow [27]. Figure 16 shows the schematic diagram of the phenomenon. In this diagram, a permanent magnet is moving vertically at a certain velocity towards a coil of wire such that an induced current is induced into the coil.

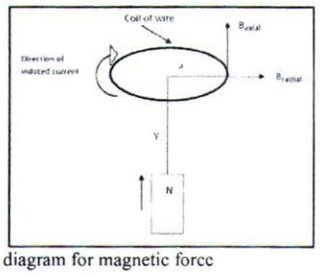

Figure 16: Schematic diagram for magnetic force

Thus, from the result obtained in Table 1, it can be surmised that the magnetic flux density (B) in the system will affect the damping coefficient (c). It has been shown that by considering aluminium as the cylindrical material in an EMD, the damping coefficient (c) of the system can be increased.

VII. CONCLUSION

In conclusion, this paper has demonstrated the effect of different materials that can be used in an EMD. The materials of nylon and aluminium have been investigated in this research. It has been shown that aluminium can generate a bigger value of damping coefficient as compared to nylon. The damping coefficient of aluminium (2.8 kgs^{-1}) is better than nylon (1.9 kgs^{-1}) because the permeability value of aluminium is greater than nylon. Thus, the interaction between the permanent magnet and the aluminium cylinder has created a bigger damping force. The output from the experimental part has been extracted and analysed with the logarithmic decrement equation. The result from the MATLAB simulation has been verified, in which the effect of the damping coefficient can be shown from the mass-spring-damper response of a vibration system.

It can be concluded that the EMD created from a permanent magnet oscillating through a specific tube does generate a damping effect. The response time for the system to damp out is affected by the type of material used in the system. This effect can be verified through the calculation of the damping value in the logarithm decrement equation.

ACKNOWLEDGEMENT

This research was funded by The National Defence University of Malaysia through the Research Grant FRGS/1/2020/STG07/UPNM/03/2.

REFERENCES

[1] Q. Cai and S. Zhu, "Enhancing the performance of electromagnetic damper cum energy harvester using microcontroller: Concept and experiment validation," *Mech. Syst. Signal Process.*, vol. 134, p. 106339, Dec. 2019, doi: 10.1016/j.ymssp.2019.106339.

[2] M. A. A. Abdelkareem *et al.*, "Vibration energy harvesting in automotive suspension system: A detailed review," *Appl. Energy*, vol. 229, no. April, pp. 672–699, Nov. 2018, doi: 10.1016/j.apenergy.2018.08.030.

[3] S. Li, J. Xu, X. Pu, T. Tao, H. Gao, and X. Mei, "Energy-harvesting variable/constant damping suspension system with motor based electromagnetic damper," *Energy*, vol. 189, p. 116199, 2019, doi: 10.1016/j.energy.2019.116199.

[4] S. Marcu, D. Popa, N. Stănescu, and N. Pandrea, "Model for the study of active suspensions," *IOP Conf. Ser. Mater. Sci. Eng.*, vol.

252, p. 012032, Oct. 2017, doi: 10.1088/1757-899X/252/1/012032.

[5] S. Gadadhe, A. More, and N. Bhone, "Experimental Analysis of Passive / Active Suspension System," *Int. Res. J. Eng. Technol.*, vol. 5, no. 11, pp. 703–707, 2018.

[6] M. R. Ahmed, A. R. Yusoff, and F. R. M. Romlay, "Adjustable Valve Semi-Active Suspension System for Passenger Car," *Int. J. Automot. Mech. Eng.*, vol. 16, no. 2, pp. 6470–6481, Jul. 2019, doi: 10.15282/ijame.16.2.2019.2.0489.

[7] M. Omar, M. M. El-kassaby, and W. Abdelghaffar, "A universal suspension test rig for electrohydraulic active and passive automotive suspension system," *Alexandria Eng. J.*, vol. 56, no. 4, pp. 359–370, Dec. 2017, doi: 10.1016/j.aej.2017.01.024.

[8] B. Ebrahimi, "Development of Hybrid Electromagnetic Dampers for Vehicle Suspension Systems," 2009.

[9] S. Kumar, A. Medhavi, and R. Kumar, "Active and Passive Suspension System Performance under Random Road Profile Excitations," *Int. J. Acoust. Vib.*, vol. 25, no. 4, pp. 532–541, Dec. 2020, doi: 10.20855/ijav.2020.25.41702.

[10] S. Li, J. Xu, X. Pu, T. Tao, H. Gao, and X. Mei, "Energy-harvesting variable/constant damping suspension system with motor based electromagnetic damper," *Energy*, vol. 189, no. April 2021, p. 116199, 2019, doi: 10.1016/j.energy.2019.116199.

[11] E. Diez-Jimenez, C. Alén-Cordero, R. Alcover-Sánchez, and E. Corral-Abad, "Modelling and Test of an Integrated Magnetic Spring-Eddy Current Damper for Space Applications," *Actuators*, vol. 10, no. 1, p. 8, Jan. 2021, doi: 10.3390/act10010008.

[12] T. M. Abdo, A. A. Huzayyin, A. A. Abdallah, and A. A. Adly, "Characteristics and analysis of an eddy current shock absorber damper using finite element analysis," *Actuators*, vol. 8, no. 4, 2019, doi: 10.3390/ACT8040077.

[13] H.-J.-J. Ho-Yeon Jung, In-Ho Kim, "Feasibility Study of the Electromagnetic Damper for Cable Structures Using Real-Time Hybrid Simulation," *sensors*, p. 2499, 2017, doi: 10.3390/s17112499.

[14] E. Diez-Jimenez, R. Rizzo, M.-J. Gómez-García, and E. Corral-Abad, "Review of Passive Electromagnetic Devices for Vibration Damping and Isolation," *Shock Vib.*, vol. 2019, pp. 1–16, Aug. 2019, doi: 10.1155/2019/1250707.

[15] Abdullah, J.-H. Ahn, and H.-Y. Kim, "Effect of Electromagnetic Damping on System Performance of Voice-Coil Actuator Applied to Balancing-Type Scale," *Actuators*, vol. 9, no. 1, p. 8, Feb. 2020, doi: 10.3390/act9010008.

[16] B. L. J. Gysen, J. J. H. Paulides, J. L. G. Janssen, and E. A. Lomonova, "Active Electromagnetic Suspension System for Improved Vehicle Dynamics," *IEEE Trans. Veh. Technol.*, vol. 59, no. 3, pp. 1156–1163, Mar. 2010, doi: 10.1109/TVT.2009.2038706.

[17] T. I. and K. A. A. J. Burhanudin, A.M. Ishak, A.S. Abu Hasim, "PERMANENT MAGNET LINEAR GENERATOR DESIGN FOR POINT ABSORBER WAVE ENERGY CONVERTER," 2019, doi: 10.1017/CBO9781107415324.004.

[18] P. Teli, V. Tamhankar, S. Zagade, and A. Suvre, "Study of Electromagnetic Damper," vol. 8, no. 09, pp. 708–711, 2019.

[19] Yong Yew Rong, "Simulation on Eddy Current Damper and its Regenerative," Universiti Tunku Abdul Rahman, 2013.

[20] H. a. Sodano, J.-S. Bae, D. J. Inman, and W. Keith Belvin, "Concept and model of eddy current damper for vibration suppression of a beam," *J. Sound Vib.*, vol. 288, no. 4–5, pp. 1177–1196, Dec. 2005, doi: 10.1016/j.jsv.2005.01.016.

[21] R. Rohith Renish, T. Niruban Projoth, K. Karthik, and K. Mohan Babu, "Vibration reduction in automobiles using electromagnetic suspension system," *Int. J. Mech. Eng. Technol.*, vol. 8, no. 8, pp. 729–737, 2017.

[22] S. Abu-Ein and S. M. Fayyad, "Electromagnetic Suspension System: Circuit and Simulation," *Int. J. Model. Optim.*, no. June 2019, pp. 440–444, 2013, doi: 10.7763/ijmo.2013.v3.316.

[23] L. A. J. Friedrich, B. L. J. Gysen, and E. A. Lomonova, "Modeling of Integrated Eddy Current Damping Rings for a Tubular Electromagnetic Suspension System," in *2019 12th International Symposium on Linear Drives for Industry Applications (LDIA)*, Jul. 2019, pp. 1–4, doi: 10.1109/LDIA.2019.8770997.

[24] K. Hyniova, "On electromagnetic actuator control in the active suspension systems," vol. 8, no. 1, pp. 6–8, 2020.

[25] P. V R, C. M. B N, and Y. S D, "Modified Electromagnetic Actuator for Active Suspension System," *Int. J. Eng. Manag. Res.*, vol. 11, no. 4, pp. 188–193, 2021, doi: 10.31033/ijemr.11.4.23.

[26] D. Kong, D. Jiang, and Y. Zhao, "Electromagnetic suspension acceleration measurement model and experimental analysis," *Electron.*, vol. 9, no. 2, pp. 1–13, 2020, doi: 10.3390/electronics9020226.

[27] S. Wayne, *Electricity, Magnetism and Light*. Academic Press, Amsterdam [etc.], 2008.

[28] J. H. Kim, Y. J. Shin, Y. Do Chun, and J. H. Kim, "Design of 100W Regenerative Vehicle Suspension to Harvest Energy from Road Surfaces," *Int. J. Precis. Eng. Manuf.*, vol. 19, no. 7, pp. 1089–1096, Jul. 2018, doi: 10.1007/s12541-018-0129-5.

[29] B. Ebrahimi, M. B. Khamesee, and F. Golnaraghi, "A novel eddy current damper: theory and experiment," *J. Phys. D. Appl. Phys.*, vol. 42, no. 7, p. 075001, Apr. 2009, doi: 10.1088/0022-3727/42/7/075001.

[30] B. L. J. Gysen, J. J. H. Paulides, J. L. G. Janssen, and E. A. Lomonova, "Active Electromagnetic Suspension System for Improved Vehicle Dynamics," *IEEE Trans. Veh. Technol.*, vol. 59, no. 3, pp. 1156–1163, Mar. 2010, doi: 10.1109/TVT.2009.2038706.

[31] Siavash Haji Akbari Fini, "Theory and Simulation of Electromagnetic Dampers for Earthquake Engineering Applications," University of British Columbia, 2016.

[32] E. Asadi, R. Ribeiro, M. B. Khamesee, and A. Khajepour, "A new adaptive hybrid electromagnetic damper: modelling, optimization, and experiment," *Smart Mater. Struct.*, vol. 24, no. 7, p. 75003, 2015, doi: Artn 075003\r10.1088/0964-1726/24/7/075003.

[33] M. Montazeri and O. Kavianipour, "Investigation of the passive electromagnetic damper," vol. 2646, no. September 2011, pp. 2633–2646, 2012, doi: 10.1007/s00707-012-0735-8.

[34] B. Ebrahimi, M. B. Khamesee, and F. Golnaraghi, "Permanent magnet configuration in design of an eddy current damper," *Microsyst. Technol.*, vol. 16, no. 1–2, pp. 19–24, 2010, doi: 10.1007/s00542-008-0731-z.

[35] A. Fow and M. Duke, "Determining the volumetric characteristics of a passive linear electro-magnetic damper for vehicle applications," *Cogent Eng.*, vol. 4, no. 1, p. 1374160, Jan. 2017, doi: 10.1080/23311916.2017.1374160.

[36] L. Zhu, C. R. Knospe, and S. Member, "Modeling of Nonlaminated Electromagnetic Suspension Systems," *IEEE Trans. Mechatronics*, vol. 15, no. 1, pp. 59–69, 2010.

[37] Z. Li, L. Zuo, G. Luhrs, L. Lin, and Y. Qin, "Electromagnetic Energy-Harvesting Shock Absorbers : Design , Modeling , and Road Tests," *IEEE Trans. Veh. Technol.*, vol. 62, no. 3, pp. 1065–1074, 2013, doi: 10.1109/TVT.2012.2229308.

[38] Q. Yang, Z. Chi, and L. Wang, "Influence and Suppression Method of the Eddy Current Effect on the Suspension System of the EMS Maglev Train," *Machines*, vol. 10, no. 6, p. 476, 2022, doi: 10.3390/machines10060476.

[39] C. C. et al. J. L. Perez-Diaz, I. Valiente-Blanco, "A novel high temperature eddy current damper with enhanced performance by means of impedance matching," *Smart Mater. Struct.*, vol. 28, no. 2, p. 025034, 2019.

[40] M. N. O. Sadiku, *Elements of Electromagnetics*, 7th editio. New York: OXFORD UNIVERSITY PRESS, 2018.

[41] B. Ebrahimi, M. B. Khamesee, and F. Golnaraghi, "Eddy current damper feasibility in automobile suspension: modeling, simulation and testing," *Smart Mater. Struct.*, vol. 18, no. 1, p. 015017, 2009, doi: 10.1088/0964-1726/18/1/015017.

[42] J. Lau *et al.*, "Advanced systems and services for ground vibration testing - Application for a research test on an Airbus A340-600 aircraft," *Proc. "IFASD 2011,"* no. January 2011, pp. 1–10, 2011, [Online]. Available: http://elib.dlr.de/70317/.

[43] T. B. Mironova, A. B. Prokofiev, and V. Y. Sverbilov, "The Finite Element Technique for Modelling of Pipe System Vibroacoustical Characteristics," *Procedia Eng.*, vol. 176, pp. 681–688, 2017, doi: 10.1016/j.proeng.2017.02.313.

[44] anurag, "Diamagnetic Materials – Definition, Properties, Applications," *geeksforgeeks.org*, 2021. Diamagnetic Materials – Definition, Properties, Applications (accessed Nov. 10, 2022).